JOURNAL OF SOLID STATE CHEMISTRY **128,** 215–219 (1997)
ARTICLE NO. SC967190

A Mixed Valent Molybdenotungsten Monophosphate with an Original Intersecting Tunnel Structure: $Li(Mo, W)_2O_3(PO_4)_2$

A. Leclaire, M. M. Borel, J. Chardon, and B. Raveau

Laboratoire CRISMAT, URA 1318 associée au CNRS, ISMRA et Université de Caen, Bd du Maréchal Juin, 14050 Caen Cedex, France

Received April 29, 1996; in revised form October 14, 1996; accepted October 15, 1996

A new molybdenotungsten monophosphate $Li(Mo,W)_2O_3(PO_4)_2$ with an intersecting tunnel structure has been synthesized. It crystallizes in the $C2/m$ space group with $a = 8.142(1)$ Å, $b = 6.361(1)$ Å, $c = 7.728(1)$ Å, $\beta = 102.45(1)°$. Its tridimensional framework consists of corner-sharing bioctahedral "M_2O_{11}" units and monophosphate PO_4 groups forming $[M_2P_2O_{15}]_\infty$ chains running along c and $[MPO_8]_\infty$ chains running along b. The $[M_2P_2O_{11}]_\infty$ framework delimits six-sided intersecting tunnels running along [110], [$\bar{1}$10], and [001], respectively. The lithium ions that are located at the intersection of these three kinds of tunnels, in the brownmillerite windows, exhibit an antiprismatic sixfold coordination. Close relationships with the two monophosphates $Mo_xW_{2-x}O_3(PO_4)_2$ and $LiMo_2O_3(PO_4)_2$ are evidenced.

INTRODUCTION

New series of mixed valent phosphates of molybdenum and tungsten, involving both elements in the same matrix, have been recently discovered. The original structures of these compounds with respect to pure molybdenum or pure tungsten phosphates are generally due to the fact that the mixed valences Mo(V)–Mo(VI) and W(V)–W(VI) behave differently. For molybdenum one often observes an ordering of the Mo(V) and Mo(VI) species, due to the particular coordination of Mo(V), whereas for tungsten an electronic delocalization is generally observed. In this respect, the introduction of an univalent cation such as lithium in a matrix of hexavalent molybdenotungsten phosphate with the formulation $(Mo, W)_2P_2O_{11}$ is of interest. The two limit phases have indeed a very different structure: the Mo(VI) phase consists of corner-sharing MoO_6 octahedra and diphosphate groups according to the formula $(MoO_2)_2P_2O_7$ (1), whereas the W(VI) phase is built up from chains of MoO_6 octahedra and monophosphate groups, according to the formulation $W_2O_3(PO_4)_2$ (2–3). Moreover, Mo(VI) and W(VI) can coexist in the second structure leading to the solid solution $Mo_xW_{2-x}O_3(PO_4)_2$ that exhibits a wide homogeneity range $0 \leq x < 1.25$ (3).

In a recent study of mixed valent molybdenum phosphates involving $[Mo_2P_2O_{11}]_\infty$ framework, two new phases were isolated. The first, $Li_xMo_2O_3(PO_4)_2$ (4), is closely related to the monophosphate $Na_x(MoW)_2O_3(PO_4)_2$ (5), whereas the second, $LiMo_2O_3(PO_4)_2$ (6), exhibits an original structure with two kinds of coordination for lithium, tetrahedral and octahedral. Thus, it appears that the exploration of systems with the formulation $Li_x(Mo, W)_2P_2O_{11}$ should allow new frameworks to be generated. The present paper deals with the synthesis and original structure of a new mixed valent molybdenotungsten monophosphate $Li(Mo, W)_2O_3(PO_4)_2$

EXPERIMENTAL

Chemical Synthesis and Crystal Growth

The synthesis of the compound $LiMo_{2-x}W_xP_2O_{11}$ for different values of x was carried out in two steps: first, $H(NH_4)_2PO_4$, Li_2CO_3, MoO_3, and WO_3 were mixed in an agate mortar in adequate ratios according to the composition $LiMo_{1.83-x}W_xP_2O_{11}$ and heated at 700 K in a platinum crucible to decompose the ammonium phosphate and lithium carbonate. In a second step, the resulting mixture was then added to the required amount of molybdenum (0.17 mole) sealed in an evacuated silica ampoule, heated for 30 hr at 873 K, cooled at 3 K per hour to 773 K, and finally quenched to room temperature. The samples obtained for $0 < x < 0.75$ were polyphased; for the compositions $0.75 < x < 1.75$ one obtains an homogeneous black polycrystalline powder. From these samples, large black crystals could easily be selected.

Elementary Analysis

The analysis of numerous crystals corresponding to different x values (0.75, 1, 1.25, and 1.50) was performed by energy dispersive analysis (EDS), using a TRACOR microprobe mounted on a scanning electron microscope JEOL J.S.M. 840. By this method the nominal cationic composition "$Mo_xW_{2-x}P_2$" was systematically confirmed. Analysis

0022-4596/97 $25.00

of lithium was performed on several crystals by atomic absorption spectroscopy using a VARIAN SpectrAA-20 spectrometer.

Single Crystal X-Ray Diffraction Study

A systematic test of the crystals extracted from the different batches, using the precession and Weissenberg techniques, showed that most of the crystals were twinned. Only the crystals extracted from the sample with composition $x = 0.75$ did not show any twinning and consequently were selected for the structure determination.

A black plate like crystal, with $0.071 \times 0.051 \times 0.019$ mm was selected for the structure determination. The cell parameters reported in Table 1 were determined and refined by diffractometric technique at 294 K with least squares refinement based upon 25 reflections with $18^\circ \leq \theta \leq 22^\circ$. The systematic absences $h + k = 2n + 1$ in whole space were consistent with the space groups *C*2, *Cm*, and *C*2/*m*. The data were collected with an Enraf Nonius CAD4 diffractometer with the parameters reported in Table 1. The reflections were corrected for Lorentz and polarization effects and for absorption and secondary extinction.

The structure was solved with the heavy atom method. The Mo and W atoms were distributed over one site *M*; the refinement of the occupancy factor of this site led to the cationic composition "$Mo_{0.68}W_{1.32}$" in agreement with the nominal composition "$Mo_{0.75}W_{1.25}P_2O_{11}$." The refinement of occupancy factor of the latter allowed occupancy 0.34(1)Mo and 0.66(1)W. Lithium atoms were then localized by Fourier difference series. The refinement of the atomic coordinates, the isotropic thermal factor of lithium, and the anisotropic thermal factor of all the other atoms was performed successfully in the space group *C*2/*m* leading to the reliability factors $R = 0.031$ and $R_w = 0.036$.

Magnetic Measurements

The magnetic susceptibility measurements were performed with a SQUID magnetometer Quantum Design in the range 100–350 K, under 1 T after zero field cooling. The sample holder signal measured under the same experimental conditions was subtracted from the measured susceptibility.

TABLE 1
Summary of Crystal Data, Intensity Measurements, and Structure Refinement Parameters for $LiMo_{0.68}W_{1.32}O_3(PO_4)_2$

Crystal data	
Space group	*C*2/*m*
Cell dimensions	$a = 8.142(1)$ Å, $b = 6.361(1)$ Å, $c = 7.728(1)$ Å $\alpha = 90.0^\circ$, $\beta = 102.45(1)^\circ$, $\gamma = 90.0^\circ$
Volume	390.8(1) Å^3
Z	2
ρ_{calc}(g cm^{-3})	4.76
Intensity measurements	
λ(Mo*K*α)	0.71073 Å
Scan mode	ω–4/3θ
Scan width (°)	$1.20 + 0.35 \tan\theta$
Slit aperture (mm)	$1.20 + \tan\theta$
Max θ(°)	45
Standard reflections	3 every hour
Reflections with $I > 3\sigma$	1342
μ (mm^{-1})	23.33
Structure solution and refinement	
Parameters refined	47
Agreement factors	$R = 0.031$ $R_w = 0.036$
Weighting scheme	$w = 1/\sigma^2$
Δ/σ_{max}	< 0.003

RESULTS AND DISCUSSION

The atomic parameters listed in Table 2 show that a new molybdenum phosphate with a novel structure has been synthesized.

The projection of the $[M_2P_2O_{11}]_\infty$ framework along **b** (Fig. 1) shows that it consists of single monophosphate groups sharing their apices with bioctahedral M_2O_{11} groups, so that the chemical formula can be written $LiMo_{0.68}W_{1.32}O_3(PO_4)_2$. The bioctahedral units are formed of two corner-shared MO_6 octahedra forming $\widehat{O–O–O}$ angles of 90°, like in the perovskite structure. Such units with the perovskite configuration are also observed in the monophosphates $Mo_xW_{2-x}O_3(PO_4)_2$ (3) and $LiMo_2O_3(PO_4)_2$ (6).

The whole structure can simply be described as the assemblage of $[M_2P_2O_{15}]_\infty$ chains running along **c** (Fig. 1). Each chain consists of bioctahedral perovskite units interconnected by two PO_4 tetrahedra, forming diamond shaped

TABLE 2
Positional Parameters and Their Estimated Standard Deviations for $LiMo_{0.68}W_{1.32}O_3(PO_4)_2$

Atom	*x*	*y*	*z*	*B*(Å^2)
M	0.15211(4)	0.0	0.21944(4)	0.37(1)
P	0.2465(2)	0.5	0.3305(2)	0.45(3)
Li	0.0	0.5	0.0	2.6(6)[a]
O(1)	0.3271(9)	0.0	0.1338(7)	1.2(1)
O(2)	0.0	0.0	0.0	0.8(2)
O(3)	0.2667(7)	0.0	0.4754(6)	0.9(8)
O(4)	0.1460(5)	0.3118(5)	0.2343(4)	0.9(7)
O(5)	−0.0745(7)	0.0	0.3130(7)	1.2(1)

Note. Anisotropically refined atoms are given in the form of the isotropic equivalent displacement parameter defined as $B = 4/3 \sum_i \sum_j \mathbf{a}_i \cdot \mathbf{a}_j \beta_{ij}$. $M = W_{0.66(1)}Mo_{0.34(1)}$.

[a] Li atom has been isotropically refined.

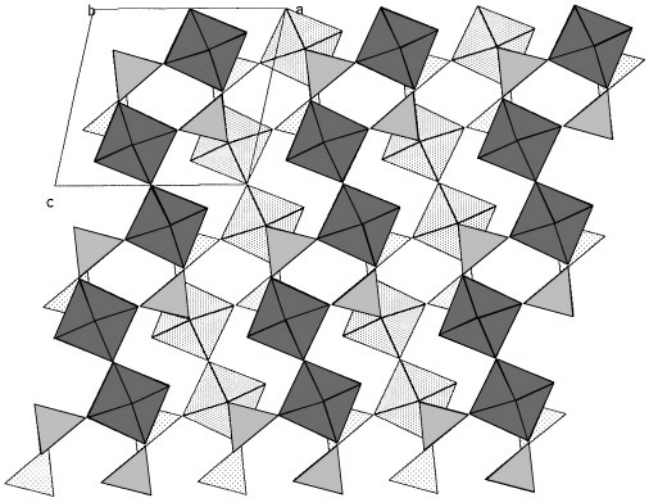

FIG. 1. Projection of the $[M_2P_2O_{11}]_\infty$ framework along **b**.

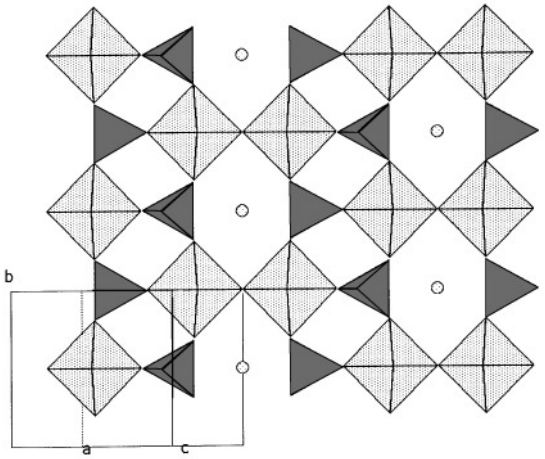

FIG. 2. $[M_4P_4O_{26}]_\infty$ layers built up from $[MPO_8]_\infty$ chains.

windows. Two successive chains at the same level ($y = 0$), are disconnected and deduced from each other by an "a" translation. Identical chains are running along **c** at the $y = 1/2$ level, but they are shifted $a/2$ with respect to the chains located at $y = 0$ (Fig. 1). As a result the apical oxygens of the MO_6 octahedra of the $y = 0$ chains are shared with oxygens of the PO_4 tetrahedra of the $y = 1/2$ chains and vice versa. Thus the tridimensional $[Mo_{0.68}W_{1.32}P_2O_{11}]$ can be described by the stacking along **b** of layers of disconnected $[M_2P_2O_{15}]_\infty$ chains. It is remarkable that practically identical layers of $[M_2P_2O_{15}]_\infty$ chains are observed in the structure of $LiMo_2O_3(PO_4)_2$ (6) and of $Mo_xW_{2-x}O_3(PO_4)_2$ (3). This similarity with two other structures explains the relationships between the cell parameters of the three structures (Table 1) that exhibit similar a and c parameters whereas the β values vary slightly due to the fact that two successive $[M_2P_2O_{15}]_\infty$ chains in a (010) layer may be slightly translated along **c** (or **a**) with respect to each other.

From the connection of the $[M_2P_2O_{15}]_\infty$ chains, it results in the formation of $[MPO_8]_\infty$ chains running along **b**. Such chains in which one PO_4 tetrahedron alternates with one MO_6 octahedron are also observed for the two other monophosphates $LiMo_2O_3(PO_4)_2$ (6) and $Mo_xW_{2-x}O_3(PO_4)_2$ (3), explaining that the b parameters of the three phases (Table 1) are similar or different by a factor two.

In fact, the three dimensional framework $[M_2P_2O_{11}]_\infty$ can be also described from the assemblage of $[MPO_8]_\infty$ chains. Considering the layers of polyhedra parallel to $(\bar{2}01)$, the entire structure results from the stacking along **a** of identical $[M_4P_4O_{26}]_\infty$ layers whose geometry is shown in Fig. 2. In such layers, each $[MPO_8]_\infty$ chain exhibits a *cis* configuration, i.e., the PO_4 tetrahedra have their fourth apices directed on the same side of the chain axis. One $[MPO_8]_\infty$ chain shares the apices of its octahedra and tetrahedra with the tetrahedra and octahedra, respectively, of the next chain on one side, and the apices of its octahedra with the octahedra of the next chain on the other side (Fig. 2). This results in brownmillerite windows similar to those encountered in $LiMo_2O_3(PO_4)_2$ (6). Two successives $[M_4P_4O_{26}]_\infty$ layers are shifted **b**/2 with respect to each other and consequently are connected in thus a way that the PO_4 tetrahedra of one layer share one apex with the MO_6 octahedra of the next layer.

It is worth pointing out that the structure of $Li(Mo, W)_2O_3(PO_4)_2$ differs fundamentally from that of $LiMo_2O_3(PO_4)_2$ (6), by the fact that in the second there exists a second kind of layer parallel to (010), also built up of $[Mo_2P_2O_{15}]_\infty$ chains but with a different geometry of the Mo_2O_{11} units, that form 60°–120° $\overline{O–O–O}$ angles. The present structure also differs from $Mo_xW_{2-x}O_3(PO_4)_2$ by the fact that the latter exhibits besides the $[MPO_8]_\infty$ chains with a *cis* configuration, the $[MPO_8]_\infty$ chain with a *trans* configuration.

The view of this tridimensional framework along [110] (Fig. 3) shows that it delimits six sided tunnels running along [110] and $[1\bar{1}0]$. In the same way the view of this structure along [001] (Fig. 4) evidences six sided tunnels running along that direction. The Li^+ cations are located at the intersection of these three tunnels, at the level of the browmillerite windows (Fig. 2).

In this $[M_2P_2O_{11}]_\infty$ framework the PO_4 tetrahedron, linked to four octahedra MO_6 by corner sharing, exhibits a regular configuration with P–O distances ranging from 1.493 to 1.547 Å (Table 3). The MO_6 octahedron linked by corner sharing with four tetrahedra and one octahedron exhibits a free apex; the two free apices of one M_2O_{11} unit are oriented in opposite directions with a *trans* configuration (Fig. 1). The MO_6 octahedra exhibit a geometry rather

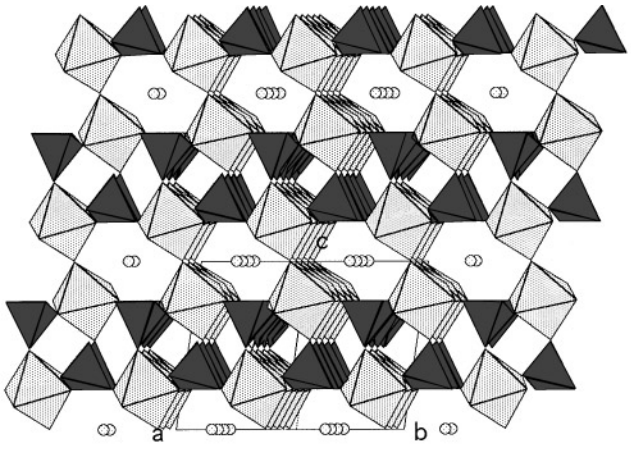

FIG. 3. View of the tridimensional $[M_2P_2O_{11}]_\infty$ framework along [110].

similar to that observed for pure Mo(V) oxides, in spite of the low molybdenum content compared to tungsten (Table 3). The shortest *M*–O bond (1.696 Å) corresponds indeed to the free oxygen atom O(1), whereas the opposite *M*–O bond is the longest (2.121 Å). The four other *M*–O distances are intermediate, corresponding to three oxygen atoms shared with PO_4 tetrahedra (1.988 to 1.997 Å) and to the bridging oxygen of the M_2O_{11} unit (1.872 Å).

The Li^+ cation exhibits a sixfold coordination forming a LiO_6 antiprism. Each LiO_6 antiprism shares two opposite edges with two PO_4 tetrahedra leading to four rather long Li–O equatorial distances of 2.279 Å (Table 3), whereas the two apical Li–O distances, that correspond to the free oxygen atom of the MO_6 octahedra, are significantly shorter (1.918 Å).

TABLE 3
Distances (Å) and Angles (°) in the Polyhedra for $LiMo_{0.68}W_{1.32}O_3(PO_4)_2$

M	O(1)	O(2)	O(3)	O(4)	O(4)^{i}	O(5)
O(1)	**1.696(6)**	2.641(5)	2.788(8)	2.684(6)	2.684(6)	3.816(7)
O(2)	95.4(2)	**1.872(1)**	3.843(7)	2.744(4)	2.744(4)	2.617(6)
O(3)	97.7(2)	166.9(2)	**1.997(5)**	2.753(5)	2.753(5)	2.791(7)
O(4)	93.2(1)	91.9(1)	87.4(1)	**1.988(4)**	3.967(7)	2.828(6)
O(4)^{i}	93.2(1)	91.9(1)	87.4(1)	172.2(2)	**1.988(4)**	2.828(6)
O(5)	177.1(2)	81.6(1)	85.3(2)	86.9(1)	86.9(1)	**2.121(6)**

P	O(5)^{ii}	O(3)^{iii}	O(4)	O(4)^{iv}
O(5)^{ii}	**1.493(6)**	2.496(8)	2.527(6)	2.527(6)
O(3)^{iii}	111.5(3)	**1.527(6)**	2.507(5)	2.507(5)
O(4)	112.5(2)	109.3(2)	**1.547(4)**	2.364(1)
O(4)^{iv}	112.5(2)	109.3(2)	101.4(2)	**1.547(4)**

Li–O(1)^{v}	1.918(6)
Li–O(1)^{vi}	1.918(6)
Li–O(4)	2.279(3)
Li–O(4)^{vi}	2.279(3)
Li–O(4)^{vii}	2.279(3)
Li–O(4)^{viii}	2.279(3)

Symmetry codes:
i: $x; -y; z$
ii: $1/2 + x; 1/2 + y; z$
iii: $1/2 - x; 1/2 + y; 1 + z$
iv: $x; 1 - y; z$
v: $x - 1/2; 1/2 + y; z$
vi: $1/2 - x; 1/2 + y; -z$
vii: $-x; 1 - y; -z$
viii: $-x; y; -z$

Note. The M–O or P–O distances are on the diagonal, above it are the O ⋯ O distances, and below it are the O–M–O or O–P–O angles.

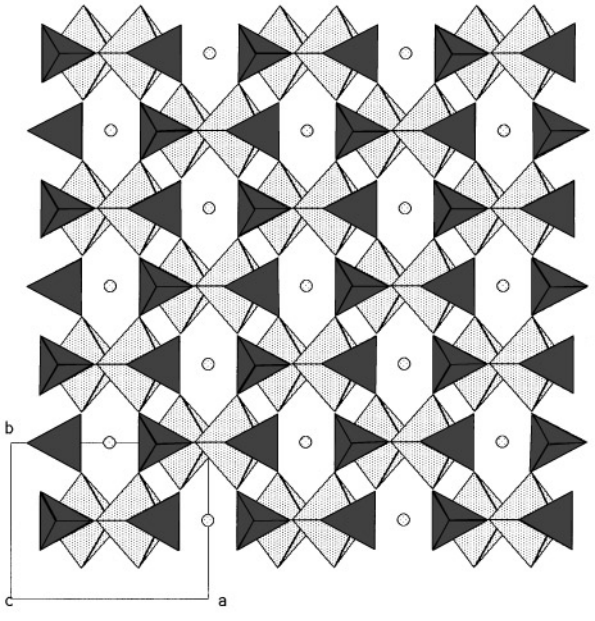

FIG. 4. View of the tridimensional $[M_2P_2O_{11}]_\infty$ framework along [001].

The reciprocal magnetic susceptibility plotted as a function of temperature (Fig. 5), between 100 and 350 K, shows paramagnetic behavior, leading to a paramagnetic moment of 1.43 μ_B per bioctahedral unit M_2O_{11}. This result is consistent with the presence of one unpaired electron per bioctahedral unit (theoretical value 1.73 μ_B) and confirms the average valence state of 5.5 per transition metal atom deduced from the chemical formula $LiMo_xW_{2-x}O_3(PO_4)_2$. One interesting issue deals with the distribution of this unpaired electron on the different atoms, forming either Mo^{5+} or W^{5+} species, or even to bioctahedral $(MoW)^{11+}$ or $(W_2)^{11+}$ species involving a delocalization of this electron between two octahedra. Energy calculations are in progress in order to shed some light on this problem.

In conclusion, this study has allowed a new mixed valent "MoW" monophosphate with an original structure to be synthesized. The close structural relationships between this phosphate and the monophosphates $Mo_xW_{2-x}O_3(PO_4)_2$

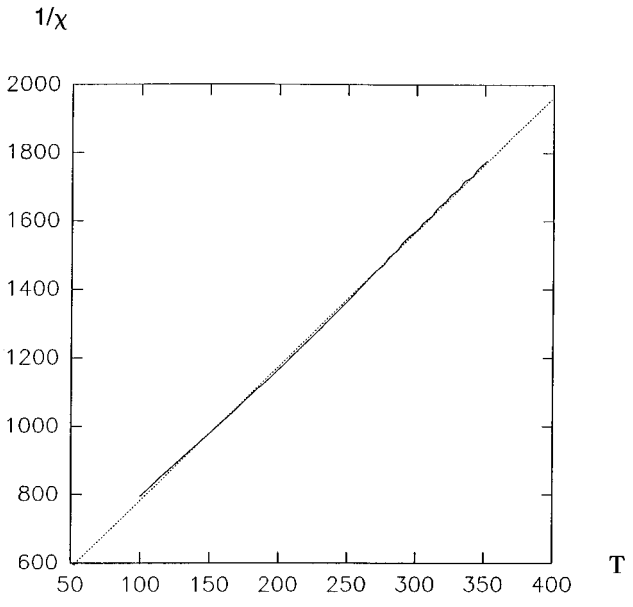

FIG. 5. $1/X_m$ versus T curve for $LiMo_xW_{1-x}O_3(PO_4)_2$.

and $LiMo_2O_3(PO_4)_2$ suggest that other lithium phosphates in the Li–Mo–W–P–O system should be generated in the future by controlling the lithium and oxygen stoichoimetry and varying the molybdenum and tungsten content.

ACKNOWLEDGMENT

We thank Dr J. Provost for the investigation of the magnetic susceptibilities of our samples.

REFERENCES

1. P. Kierkegaard, *Ark. für Kemi.* **19** (1962).
2. P. Kierkegaard, *Acta Chem. Scand.* **14,** 657 (1960).
3. A. Leclaire, M. M. Borel, J. Chardon, and B. Raveau, submitted for publication.
4. S. Ledain, A. Leclaire, M. M. Borel, and B. Raveau, *J. Solid State Chem.* **122,** 107 (1996).
5. A. Leclaire, M. M. Borel, J. Chardon, and B. Raveau, *J. Solid State Chem.* **120,** 353 (1995).
6. S. Ledain, A. Leclaire, M. M. Borel, and B. Raveau, *J. Solid State Chem.* **124,** 322 (1996).